INTRODUCTION TO RF LINEAR ACCELERATORS (LINACS)[1)]

P.M. Lapostolle

Abstract
The history of linear accelerators is now more than 50 years old and after a difficult start presented many remarkable successes. Theory and technology encounter difficult problems briefly presented here with the solutions so far developed on orbit stability, focusing, RF structure and beam dynamics computations. Questions still remain however about high intensity limits which, when answered, might still open a more brilliant future for these types of machine.

1. BRIEF HISTORY OF LINACS

The first accelerators built for nuclear physics were of electrostatic type; such machines were efficient but limited in voltage due to electrical breakdown.

In 1924 a proposal was made by Ising to add several accelerations without having anywhere the total voltage.
The method was based on the use of *drift tubes* and time varying fields, as sketched in Fig. 1.

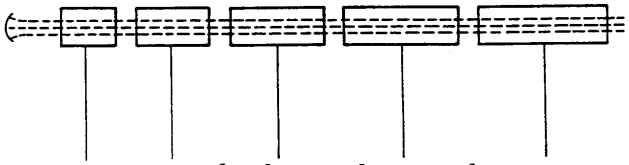

Fig. 1 Drift tube accelerator of Ising

Along the axis of metallic tubes, charged particles can drift without being subject to any electric field except at their ends, in the gaps between two consecutive drift tubes, according to their respective voltage *V*. If an accelerating voltage is applied initially to all the tubes and is switched off on each of them between the time of entrance and exit of a charged particle, the particle will receive in each gap a succession of accelerations. In practice, voltage pulses are more appropriate, as used in present day *induction linacs*; needless to say, however, that at the time of the proposal shape and timing of high voltage pulses were not good enough to produce a useful operation.

In 1928, Wideröe proposed to replace voltage pulses by an RF voltage (with a constant frequency, the drift tube lengths have to increase with the β of the particles). The method was tested on a single drift tube (input + output) and with 25 kV RF peak voltage, it was possible to observe an acceleration of 50 keV for singly-charged Na and K ions.

In 1931 Sloan and Lawrence built a real linac of 30 drift tubes giving to Hg ions an energy of 1.25 MeV; lengthening it later in 1934 to 36 drift tubes and increasing their voltage they reached 2.8 MeV. the intensity was of course very low and the beam quality not specified: R.F. voltage differed from Ising pulses, having no real flat top, phase stability (see Section 2) was not yet discovered and focusing was not ensured, except maybe by ES lens effect (see Section 5).

No further development occurred until the war, due to the lack of proper high power RF technology (limited then to 10 MHz) and to the discovery of the cyclotron. The length of the Sloan and Lawrence machine approached 2 m with a β_{max} of only a few thousandths; with the

---

1) More details on the subject can be found in a Los Alamos report LA 11601 MS, Proton Linear Accelerators, or in a CERN Yellow Report (in French) CERN 87-09

same RF wavelength of 30 m acceleration of protons would have led to a prohibitive length. In cyclotrons, on the contrary, the spiralling of the trajectories together with some focusing effect allowed the succession of many accelerations over a limited extent, leading to the possibility of producing 10 MeV protons.

The development of radars offered, after the war, pulsed high voltage equipment in the metric and centimetric wave ranges; science and technology of electromagnetism and beam dynamics of already high level were then available.

The parallel development of circular accelerators (synchrocyclotrons and synchrotrons) was also helpful with the discovery of phase stability.

Ginzton, Hansen, Chodorow, Slater, Walkinshaw used 3 GHz to accelerate electrons.

Alvarez and Panofsky used 200 MHz for protons.

2. LONGITUDINAL MOTION. PHASE STABILITY. ACCELERATION BY A TRAVELLING WAVE

For a given geometry of the drift tubes which corresponds to a certain rate of acceleration, particles must receive at each gap an exact energy gain and the voltage must have an exact value. The RF voltage V applied is larger and there are two phases per RF period for which the voltage has the right value V_S (see Fig. 2). When the field is rising the phase is stable since a particle arriving too early will be less accelerated and slip slightly in phase until the next gap; vice versa for a late particle. The other phase is unstable. The stable phase is called the *synchronous phase* ϕ_S and one has

$$V_s = V\cos\varphi_s$$

with $\phi = 0$ corresponding to the crest (proton case).

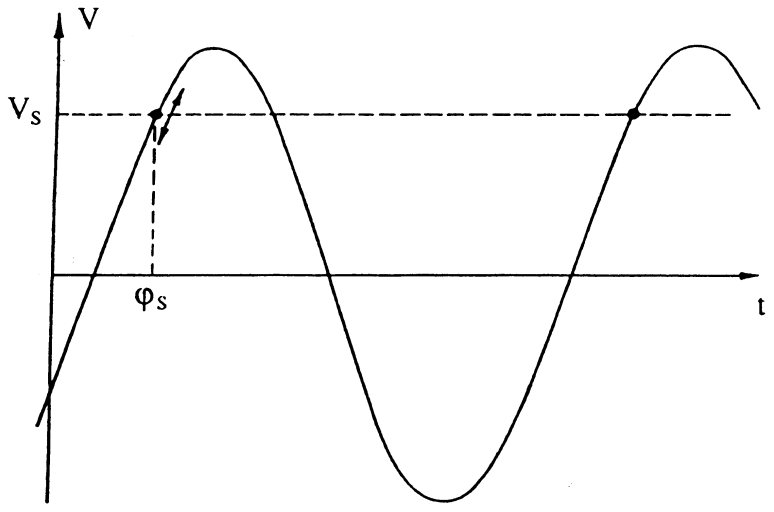

Fig. 2 Phase instability

In a first approach one can replace the discrete gap configuration by an equivalent continuous interaction (in Section 5 will appear a justification). One may say that the field distribution along the axis in the successive gaps presents an analogy with a standing wave pattern, sum of a forward and a backward wave. One would then consider the interaction of the forward synchronous wave with the particles.

Introducing relativity symbols and letting $\varphi_s,\ \beta_s,\ \gamma_s$ refer to the synchronous particle, one has

$$\gamma = 1 + \frac{W}{m_0 c^2}$$

and putting

$$\delta\gamma = \gamma - \gamma_s$$

one can write, following the path of a particle, along the axis

$$\frac{m_0 c^2}{w}\frac{d(\delta\gamma)}{ds} = \frac{qET}{w}(\cos\varphi - \cos\varphi_s)$$

$$\frac{d\varphi}{ds} = \frac{\omega}{c}\left(\frac{1}{\beta} - \frac{1}{\beta_s}\right) = -\frac{\omega}{c}\frac{\delta\gamma}{\beta_s^3\gamma_s^3}$$

whence

$$m_0 c^3 \frac{d}{ds}\left(\frac{\beta_s^3\gamma_s^3}{\omega}\frac{d\varphi}{ds}\right) = -qET(\cos\varphi - \cos\varphi_s)$$

Forgetting about the change in γ_s one then obtains

$$\delta\gamma^2 + \frac{2qET\beta_s^3\gamma_s^3}{\omega m_0 c}(\sin\varphi - \varphi\cos\varphi_s) = C^t$$

where *ET* is the amplitude of the synchronous wave.

Such a motion derives from the Hamiltonian

$$H = -\frac{\omega}{c}\frac{\delta\gamma^2}{2\beta_s^3\gamma_s^3} - \frac{qET}{m_0 c^2}(\sin\varphi - \varphi\cos\varphi_s)$$

Neglecting the change in γ_s is only valid for heavy particles (protons and ions) for which it is slow enough. It corresponds to an acceleration fighting against a constant breaking force (or to a forced pendulum model as often presented for circular machines).

One gets from it the usual stability bucket of Figs. 3 and 4; Fig. 5 shows the phase space plot relative to an operation with $\varphi_s = 0$ (fixed point as used by Sloan and Lawrence).

Taking into account the change in γ_s opens up the bucket and gives the so-called golf club, see Fig. 6 (notice that the coordinates used are not conjugate).

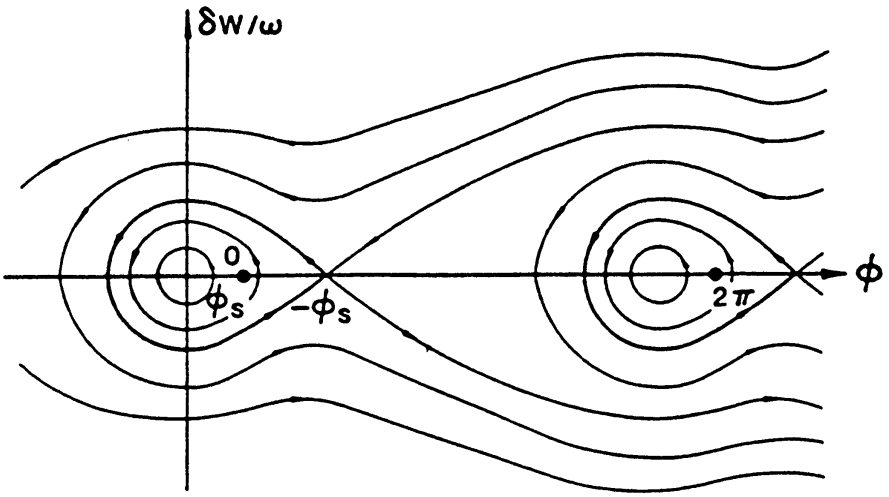

Fig. 3 Classical stability bucket

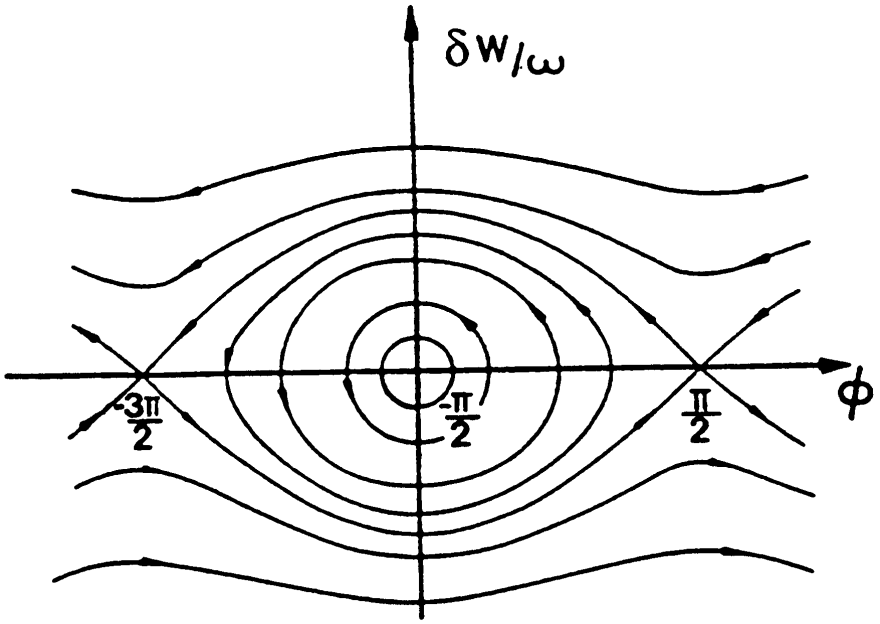

Fig. 4 Non-accelerating bucket

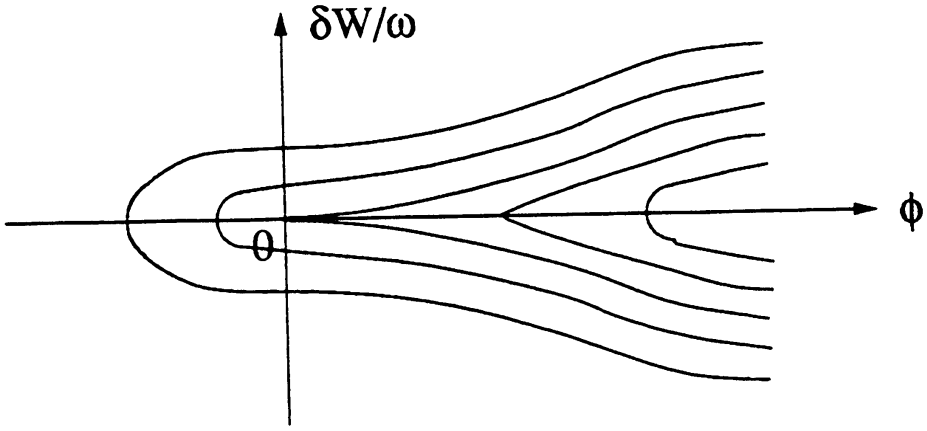

Fig. 5 Fixed-point operation

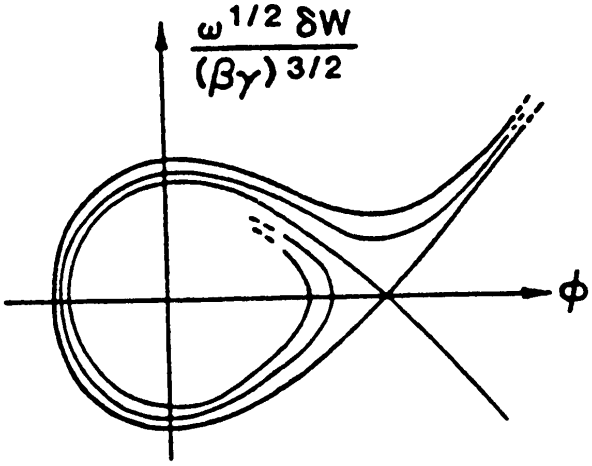

Fig. 6 Golf club

For electrons γ increases very rapidly and β becomes close to 1 over a short distance. Most of the accelerating structure (apart from a buncher) is a constant velocity $\beta = 1$ structure.

The previous derivation must be modified; keeping γ instead of $\delta\gamma$, it leads to:

$$\sqrt{\frac{1-\beta}{1+\beta}} = \gamma - \sqrt{\gamma^2 - 1} = \frac{eET}{\omega m_0 c}\left(\cos\varphi - \cos\varphi_0\right)$$

where φ refers now to a 0 of the field expressed as ET sin φ (electron linac convention). Figure 7 shows a corresponding phase space plot. One may notice that the φ_0 of a curve corresponds to its position for $\gamma \to \infty$.

Introducing, as is the custom

$$\alpha = \frac{eET\lambda}{m_0 c^2} = 2\pi\frac{eET}{\omega m_0 c}$$

one can see that for $\alpha \geq 2\pi$ the curve corresponding to $\varphi_0 = \pi/2$ which provides the maximum acceleration can start from $W = 0$. For $\alpha < \pi$, however, there can be low energy electrons just slipping in phase and not accelerated (Fig. 7).

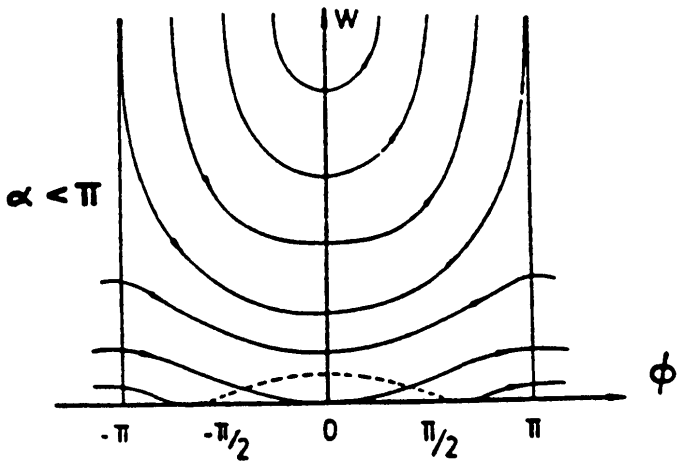

Fig. 7 Electron acceleration phase plot for $\alpha < \pi$

3. TRANSVERSE MOTION. DEFOCUSING ACTION OF THE ACCELERATING FIELD

The fields at the entrance and exit of a gap produce focusing and defocusing actions (see Fig. 8). If the field is rising the overall effect is defocusing.

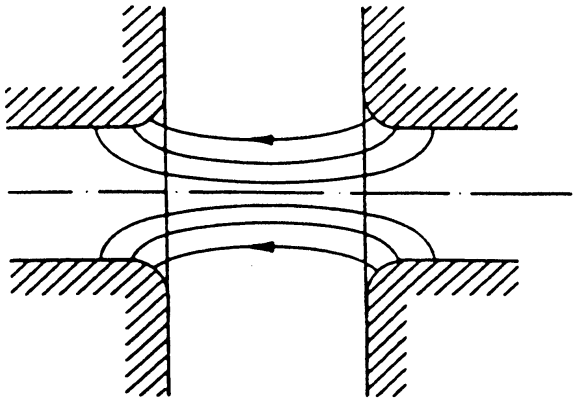

Fig. 8 Focusing and defocusing actions in a gap

Calling on the travelling wave accelerator concept one may transform the EM field of the synchronous wave in a frame moving at the same velocity (supposed constant). A TM accelerating field becomes electrostatic. Then

$$\frac{\partial E_z}{\partial z} = -\frac{\partial E_x}{\partial x} - \frac{\partial E_y}{\partial y} = -2\frac{\partial E_r}{\partial r}$$

If there is a longitudinal stability in z, there is instability in the transverse direction.

This has been a strong handicap for ion linacs until AG focusing was invented and applied (thin foils were destroyed by breakdown and thick wire grids, if transparent enough, introduced bad aberrations). New methods exist now, in particular the RFQ principle for low β.

For electrons, which become very quickly relativistic, the transverse effects are very weak.

4. LINAC ACCELERATING STRUCTURES

(Only a general review is given here; details can be found in more specialized lectures, in particular on ion linacs.)

In a circular waveguide, the phase velocity of the waves β_{ph} is always larger than 1. It is then necessary to slow them down. Periodic loading is used and/or field concentration or reorientation via drift tubes.

The structure must also provide space to install quadrupole focusing (at least at low β for ions and protons).

Stability of the field distribution is also a concern.

$\beta << 1$ (ions)

Sloan and Lawrence structure (present design, see Fig. 9a); the large drift tubes can house quadrupoles (frequency from 10 to 100 MHz).

H-type structure (see Fig. 9b); the field of the transverse electric mode is made accelerating through the drift tube configuration; since there is not much space for focusing, the fixed point operation (see Fig. 5) is used, with focusing and rebunching from place to place (frequency up to 100 MHz).

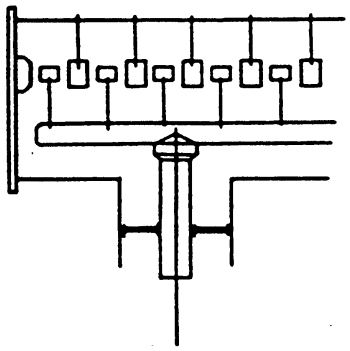

Fig. 9a

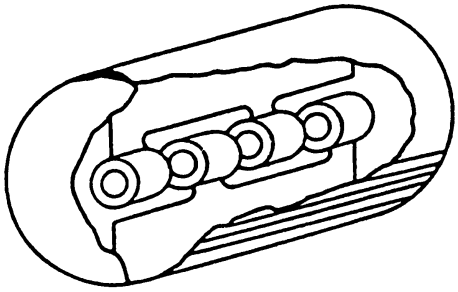

Fig. 9b

<u>$0.02 < \beta < 0.1$</u>

Quasi Alvarez structure (see Fig. 10); the large drift tubes (almost $2\beta\lambda$ long) can house quadrupoles; the rate of acceleration is lower than with the H-type structure (frequency up to 200 MHz); high intensities can be accelerated.

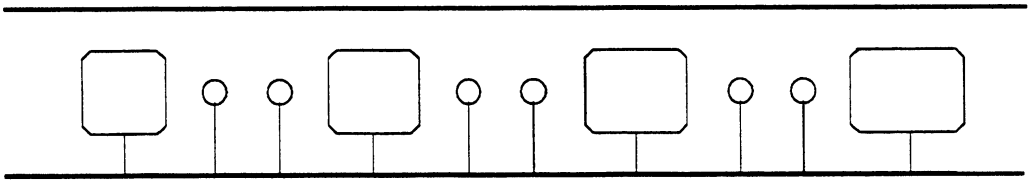

Fig. 10

<u>$0.03 < \beta < 0.4$</u>

Alvarez structure (most common for protons, see Fig. 11); a quadrupole is put in each drift tube. Such a structure allows very large intensities (frequency between 100 and 400 MHz). For β approaching 0.5 the RF losses increase, the drift tubes becoming resonant like $\lambda/2$ antenna.

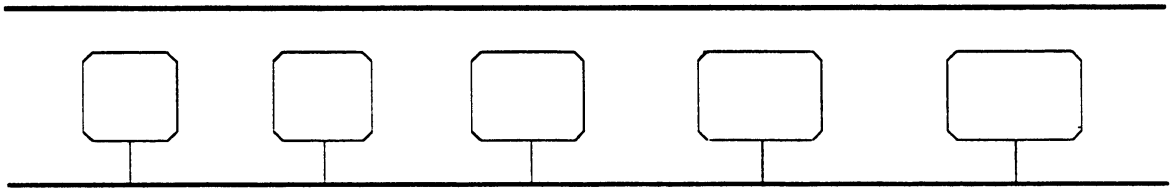

Fig. 11

<u>$\beta > 0.4$ (protons)</u>

Side-coupled cavities (Fig. 12). At this β the focusing is installed in between sections of cavities (frequency from 600 to 1200 MHz).

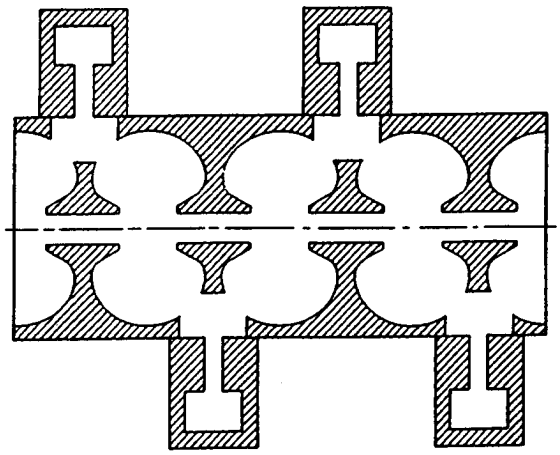

Fig. 12

β = 1 (electrons)

Iris-loaded cavity (Fig. 13) with three or four irises per wavelength λ (frequency usually 3 GHz).

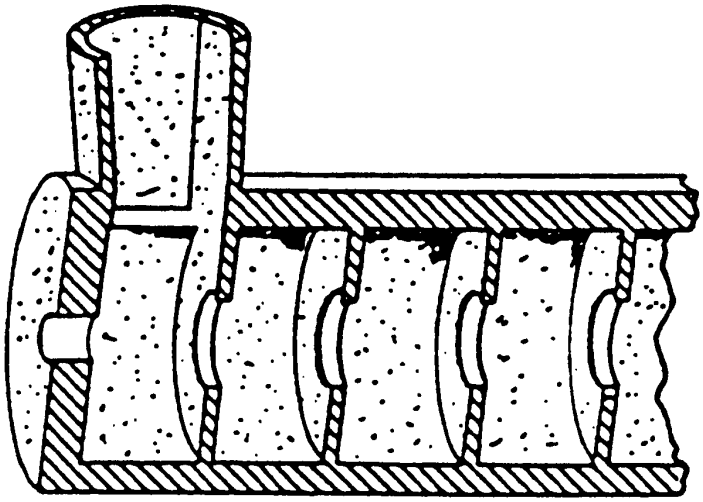

Fig. 13

Other types of structures

Superconducting (or normal temperature) independent cavities for heavy-ion boosters: a few gaps or even a helix. Very flexible for various particles and different β: for each velocity and particle (charge and mass) the phase of the independent cavities is correspondingly adjusted.

RFQ (low-β protons and ions): cavity excited on a quadrupolar EM mode with profiled vanes or rods to provide acceleration.

5. DETAILED PARTICLE DYNAMICS COMPUTATION

Acceleration through a gap
Transit time factor
Simulation codes

The initial approach (Panofsky equations) was developed from the experience gained on electron beam tubes with grids (see Fig. 14). In the case of grids the field in a gap can be uniform of value E_0. With open holes on the contrary it penetrates inside and can have, on the axis, a distribution as shown on the figure.

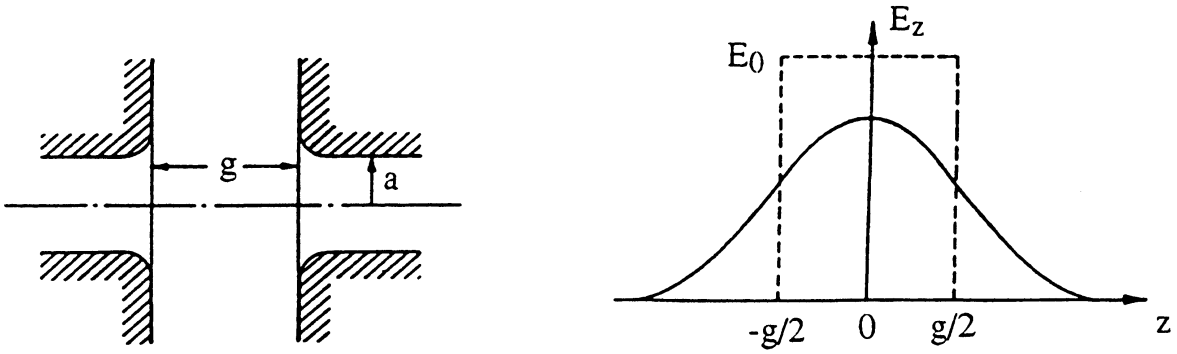

Fig. 14 Accelerating gap

With the initial approach (with grids) if one assumes a particle crosses the gap with a constant velocity v with the phase φ in the middle, the energy gain is:

$$\Delta W = q \int_{-g/2}^{+g/2} E_0 \cos\left(\frac{\omega z}{v} + \varphi\right) dz = qVT \cos\varphi$$

with

$$V = E_0 g$$

voltage across the gap, and

$$T = \frac{\sin \theta/2}{\theta/2}$$

where

$$\theta = \omega g / v$$

θ is the transit time (in phase) through the gap and T is called the transit time factor (always < 1): it is the reduction in acceleration with respect to what the voltage V would give.

In the real case (without grids) it is possible to express the amplitude of the field $E_z(z)$ on the axis (as obtained from measurements or rather from a computer) with the help of a Fourier integral:

$$E_z(z, r=0) = \frac{V}{2\pi} \int_{-\infty}^{+\infty} T(k_z) \cos k_z z \; dz$$

with the inverse relation

$$VT(k_z) = \int_{-\infty}^{+\infty} E_z(z,0) \cos k_z z \; dz$$

from which

$$V\frac{dT(k_z)}{dk_z} = -\int_{-\infty}^{+\infty} zE_z(z,0) \sin k_z z \; dz$$

In such an expression the field is represented as the sum of an infinite set of travelling waves of amplitude proportional to $T(k_z)$ (in a standing wave configuration only two waves are present). Each wave $T(k_z)$ is an EM wave the complete distribution of which can be known from Maxwell's equation (assuming circular symmetry) in such a way that the complete field distributions can be derived throughout the gap inside of a cylinder of radius a, the hole radius:

$$E_z(z,r,t) = \frac{V}{2\pi}\int_{-\infty}^{+\infty} T(k_z) I_0(k_r r) \cos k_z z \cos(\omega t + \varphi) dk_z$$

$$E_r(z,r,t) = \frac{V}{2\pi}\int_{-\infty}^{+\infty} T(k_z)\frac{k_z}{k_r} I_1(k_r r) \sin k_z z \cos(\omega t + \varphi) dk_z$$

$$cB_\theta(z,r,t) = \frac{V}{2\pi}\int_{-\infty}^{+\infty} T(k_z)\frac{w}{ck_r} I_1(k_r r) \cos k_z z \sin(\omega t + \varphi) dk_z$$

with

$$k_r^2 = k_z^2 - \omega^2 / c^2$$

With such expressions, making use of inverse Fourier relations, one can easily compute the energy gain. Along a parallel to the axis, at the distance r, one has:

$$\Delta W = qVT(k_z) I_0(k_r r) \cos \varphi$$

where $k_z = \omega/v_\phi$ and $T(k_z)$ is the amplitude factor relative to the synchronous wave; the fact that only the synchronous wave interacts justifies the approach used in Section 2. It also explains a correction often introduced in the expression of the transit time, as follows:

$$T = \frac{\sin \theta/2}{\theta/2}\frac{I_0(k_r r)}{I_0(k_r a)}$$

with, for θ, a slight correction to take into account the effect of the chamfer of the hole.

With the field equations above one can compute the phase change across the gap, accounting for the change in velocity, and the transverse motion. It is also possible to consider a trajectory with a slope, such that

$$r = r_0 + r_0' z$$

Such integrals lead to expressions involving $T(k_z)$ and its first and second derivatives with respect to k_z, according to the relation given above (see the report LA-11601-MS, page 80).

These expressions are used in common codes like PARMILA and MAPRO, valid however only for protons and ions.

A more recent code, DYNAC, valid for all particles (including electrons), with a better accuracy, introduces instead of the radius r the reduced radius

$$R = r\sqrt{\beta z} \quad \text{with} \quad R' = \frac{dR}{dz}$$

leading, in the paraxial approximation, to:

$$R'' - R\frac{q}{2m_0c^3}\frac{1}{\beta^3\gamma^3}\frac{\partial E_z}{\partial t} + R\left(\frac{q}{2m_0c^2}\right)^2\frac{\gamma^2+2}{\beta^4\gamma^4}E_z^2 = 0$$

such that R and R' are conjugate (which was not the case for r and r').

This equation shows, in addition to the phase dependent term usually defocusing (see Section 3), a focusing term of the electron lens type, mainly important for electrons but also for very low velocity particles (explaining probably the weak focusing observed by Sloan and Lawrence, see Section 1).

Such a term for a uniform field just leads by integration to the classical solution and the relation between r and R; it can however in the case of localized fields (gaps) exhibit an appreciably enhanced effect, not at all in contradiction with the considerations developed in a moving frame at *constant* velocity.

The derivation of the equation in R, not given in the report LA-16601-MS, is developed in the Appendix.

6. SPACE CHARGE EFFECTS. INTENSITY LIMITS

Particles of the same charge repel each other. Space charge field tends to increase the beam size and hence entails a risk of loss.

According to Poisson's law a linear space charge field requires ρ = Cte.

The only solution for a uniform density, only possible for a continuous beam is the so-called Kajchinsky-Vladimirsky (K.V.) distribution, which is a surface distribution in the 4D space. Such a distribution is, of course, not very physical but fortunately it happens, from energy consideration, that the K.V. beam equations are satisfied approximately (over short enough distances) by r.m.s. dimensions (size and emittances) for all distributions (for a K.V. distribution r.m.s. dimensions are half the real ones and r.m.s. emittances one quarter of the real ones). Such a property is extremely useful, in simulation studies for instance, for finding good matching conditions.

When the intensity increases, various phenomena occur, due to the non-linear character of space charge forces.
Beam emittance can transfer from one coordinate to another and total emittance tends to increase.

Around the beam core a "halo" develops; when trying to scrape it, it reappears. Even if such a halo contains only one or a few per cent of the particles or even less this can be a very serious problem for large intensity machines.

For small average intensity on the other hand, the emittance (beam quality) is the main concern. A practical recipe which leads to good operation is as follows:

AG focusing is usually specified by the phase advance per focusing period of the incoherent oscillations; calling σ_0 the value for zero intensity and σ for full beam one must have $\sigma_0 < 90^\circ$ and usually σ_0 in the range of 60 or 70° with $\sigma/\sigma_0 > 0.4$.

In addition focusing and longitudinal stability should be adjusted, as far as possible, in such a way that transverse kinetic energy and longitudinal oscillation energy remain as close as possible to avoid emittance transfer.

Several simulation codes are available to study numerically the space charge effects. The beam is represented by a few thousand of macroparticles and several methods are used to compute their space charge field:

A fast Fourier transform (FFT) routine to solve Poisson's law when one can assume a circular symmetry for the bunch (PIC, particle in cell code)

A numerical integration using analytical expressions valid for an ellipsoidal bunch shape (Ellipsoidal profile code)

A point-to-point computation which does not make any assumption on the geometry but requires some care to avoid "collisional effects" (Particle-to-particle interaction code); this last code is much slower when increasing the number of macroparticles.

Present theoretical approaches to study the details and analyze the phenomena strongly related to highly non-linear space charge fields are making use of the modern theories of stochasticity with resonance overlap effects and Arnold's diffusion. They are still under development.

BIBLIOGRAPHY

G. Ising, Ark. Mat. Astron. Fyz. 18 (1924) 1.

R. Wideröe, Archiv für Electrotechnik 21 (1928) 387.

D.H. Sloan and E.O. Lawrence, Phys. Rev. 38 (1931) 2021.

D.H. Sloan and W.M. Coates, Phys. Rev. 46 (1934) 539.

L. Alvarez, The design of a proton linear accelerator, Phys. Rev. 70 (1946) 799.

J.P. Blewett, Phys. Rev. 88 (1952) 1197.

L. Alvarez et al., Berkelez proton linear accelerator, Rev. Sci. Instrum. 26 (1955) 111 and 210.

V.I. Veksler, A new method of acceleration, J. Phys. USSR 9 (1945) 153.

I. Kapchinskij and V. Vladimirskij, Proc. Int. Conf. on High Energy Accelerators, Geneva, 1959 (CERN, Geneva, 1959), p. 274.

E.M. MacMillan, The synchrotron, Phys. Rev. 68 (1945) 143.

L. Smith, Linear accelerators, Handbuch der Physik, Band XLIV (Springer, Berlin, 1959), p. 341-389.

H. Bruck, Accélérateurs circulaires de particules (Presses Univ.de France, Paris, 1966). [English translation by Los Alamos: Circular particle accelerators, LASL.LA TR 72-10 Rev. (1972).]

A. Lichtenberg, Phase space dynamics of particles (J. Wiely and Sons, New York, 1969).

E. McMillan, The relation between phase stability and first order focusing, Phys. Rev. 80 (1950) 493.

L. Teng, AG focusing for linacs, Rev. Sci. Instrum. 25 (1954) 264.

L. Smith et al., Focusing in linacs, Rev. Sci. Instrum. 26 (1955) 220.

E. Nolte et al., The Munich heavy ion post accelerator, IEEE Trans. Nucl. Sci. NS-26 (1979) 3724.

T. Fukushima et al., Measurement of interdigital H type linac, Proc. Linear Accelerator Conf., Santa Fe, 1981 (LA 9234C, Los Alamos, 1982), p. 296.

E. Knapp et al., Standing-wave high-energy linacs, Rev. Sci. Instrum. 39 (1968) 979-991.

D. Böhne, The UNILAC, Proc. Linear Accelerator Conf., Chalk River, 1976 (AECL 5677, Chalk River, 1976), p. 2.

L. Smith, Beam dynamics in induction linacs, Proc. Linear Accelerator Conf., Santa Fe, 1981 (LA 9234C, Los Alamos, 1982), p. 111.
T. Fessenden, Induction linacs for HIF, Proc. Linear Accelerator Conf., Seeheim, 1984 (GSI 84-11, Darmstadt, 1984), p. 485.

A. Schempp et al., A heavy ion post accelerator, Proc. Linear Accelerator Conf., Montauk, 1979 (BNL 51134, Brookhaven, 1980), p. 159.

L. Bollinger et al., Concept of a superconducting linac, Proc. Linear Accelerator Conf., Seeheim, 1984 (GSI 84-11, Darmstadt, 1984), p. 217.

I. Kapchinskij et al., The linac with space uniform quadrupole focusing, IEEE Trans. Nucl. Sci. NS-26 (1979) 3462.

J. Potter et al., RFQ research at Los Alamos, IEEE Trans. Nucl. Sci. NS-26 (1979) 3745.

R. Stokes et al., RFQ dynamics, IEEE Trans. Nucl. Sci. NS-26 (1979) 3469.

K. Halbach et al., Properties of the code SUPERFISH, Proc. Linear Accelerator Conf., Chalk River, 1976 (AECL 5677, Chalk River, 1976), p. 122, and SUPERFISH, Part. Accel. 7, (1976) 213.

M. Bell et al., Numerical computation of field distribution, Proc. Linear Accelerator Conf., Batavia, 1970 (NAL, Batavia, 1971), p. 329.

W. Panofsky et al., Berkeley proton linac, Rev. Sci. Instrum. 26 (1955) 119.

P. Lapostolle, Equations de la dynamique des particules, rapport CERN AR/Int. SG5/11 (1965).

A. Carne et al., Design equations in a linac, Proc. Linear Accelerator Conf., Los Alamos, 1966 (LA 3609, Los Alamos, 1966), p. 201.

M. Promé and M. Martini, Computer studies of beam dynamics, Part. Accel. 2 (1971) 289-299.

I. Hofmann, Generalized three-dimensional equations for the emittance and field energy of high-current beams in periodic focusing structures, Part. Accel. 21 (1987) 69.

P. Lapostolle, Relations énergétiques dans les faisceaux continus, rapport CERN ISR DI/71-6 (1971). [English translation by Los Alamos: LA TR 80-8 (1980.]

F. Sacherer, r.m.s. envelope equations with space charge, IEEE Trans. Nucl. Sci. NS-18 (1971) 1105.

T. Wangler, Relation between field energy and r.m.s. emittance, IEEE Trans. Nucl. Sci. NS-32 (1985) 2196.

D. Warner, Accelerating structure of CERN Linac, Proc. Linear Accelerator Conf., Chalk River, 1976 (AECL 5677, Chalk River, 1976), p. 49.

M. Weiss, The new CERN Linac, Proc. Linear Accelerator Conf., Montauk, 1979 (BNL 51134, Brookhaven, 1980), p. 67.

R. Chasman, Numerical calculation of transverse emittance growth, IEEE Trans. Nucl. Sci. NS-16 (1969) 202.
R. Jameson, Equipartitioning in linacs, Proc. Linear Accelerator Conf., Santa Fe, 1981 (LA 9234C, Los Alamos, 1982), p. 125.

P. Lapostolle, Etude numérique de charge d'espace, rapport CERN ISR/78-13 (1978).

APPENDIX

EQUATION OF THE TRANSVERSE MOTION WITH THE REDUCED RADIUS IN THE PARAXIAL APPROXIMATION

The equation

$$\frac{d(mv_r)}{dt} = q(E_r - v_z B_\theta) \tag{A.1}$$

can be written

$$d(r'\beta\gamma) = \frac{q}{m_0 c}(E_r - \beta c B_\theta)dt = k(r,z,t)dt \tag{A.2}$$

Putting

$$R = r\sqrt{\beta\gamma} = r\left(\gamma^2 - 1\right)^{1/4} \quad \text{and} \quad R' = dR/dz \tag{A.3}$$

one has

$$r' = R'\left(\gamma^2 - 1\right)^{-1/4} - \frac{R}{2}\gamma\left(\gamma^2 - 1\right)^{-5/4}\frac{d\gamma}{dz} \tag{A.4}$$

and

$$\begin{aligned}\frac{d}{dz}(r'\beta\gamma) = {} & R''\left(\gamma^2 - 1\right)^{1/4} \\ & + \left[-\frac{R}{2}\left(\gamma^2 - 1\right)^{-3/4} + \frac{3R}{4}\gamma^2\left(\gamma^2 - 1\right)^{-7/4}\right]\left(\frac{d\gamma}{dz}\right)^2 \\ & - \frac{R}{2}\gamma\left(\gamma^2 - 1\right)^{-3/4}\frac{d^2\gamma}{dz^2}\end{aligned} \tag{A.5}$$

Now, from Eq. (A.2), in the paraxial approximation

$$k(r,z,t) = k(z,t)r = \frac{q}{m_0 c}\left(\frac{\partial E_r}{\partial r} - \beta c\frac{\partial B_\theta}{\partial r}\right)\cdot r \tag{A.6}$$

with, according to Maxwell's equations

$$\frac{\partial E_r}{\partial r} = -\frac{1}{2}\frac{\partial E_z}{\partial z} \quad \text{and} \quad \frac{\partial B_\theta}{\partial r} = \frac{1}{2c^2}\frac{\partial E_z}{\partial t} \tag{A.7}$$

But one has from Eq. (A.2)

$$\frac{d}{dr}(r'\beta\gamma) = \frac{k(r,z,t)}{\beta c} \tag{A.8}$$

and, for the longitudinal motion

$$m_0 c^2 \frac{d\gamma}{dz} = qE_z \tag{A.9}$$

so that one also has

$$m_0 c^2 \frac{d^2\gamma}{dz^2} = q\frac{dE_z}{dz} = q\frac{\partial E_z}{\partial z} + \frac{q}{\beta c}\frac{\partial E_z}{\partial t} \tag{A.10}$$

Eventually one obtains

$$\frac{d^2R}{dz^2} - R\frac{q}{2m_0c^3}\frac{1}{\beta^3\gamma^3}\frac{\partial E_z}{\partial t} + R\left(\frac{q}{2m_0c^2}\right)^2 \frac{\gamma^2+2}{\beta^4\gamma^4}E_z^2 = 0$$